An Emerging Role of Sonic Hedgehog Shedding as a Modulator of Heparan Sulfate Interactions*5

Received for publication, October 25, 2012 Published, JBC Papers in Press, November 1, 2012, DOI 10.1074/jbc.M112.356667

Stefanie Ohlig^{‡1}, Ute Pickhinke^{‡1}, Svetlana Sirko[§], Shyam Bandari[‡], Daniel Hoffmann[¶], Rita Dreier[‡], Pershang Farshi[‡], Magdalena Götz[§], and Kay Grobe[‡]

From the [†]Institute for Physiological Chemistry and Pathobiochemistry, University Hospital Münster, Waldeyerstrasse 15, D-48149 Münster, Germany, the §Institute for Physiological Genomics, Ludwig-Maximilians-Universität, Pettenkoferstrasse 12, D-80336 Munich, Germany, and the [¶]Center for Medical Biotechnology, University of Duisburg-Essen, Universitätsstrasse 1-5, D-45117 Essen, Germany

Background: Sonic hedgehog is released from expressing cells by proteolytic cleavage (shedding) of lipidated N-terminal

Results: The heparan sulfate (HS) binding Cardin-Weintraub motif represents one N-terminal protease cleavage site in vitro and in vivo.

Conclusion: This results in impaired HS binding of solubilized proteins.

Significance: Shedding may facilitate Sonic hedgehog diffusion through the HS-rich extracellular matrix.

Major developmental morphogens of the Hedgehog (Hh) family act at short range and long range to direct cell fate decisions in vertebrate and invertebrate tissues. To this end, Hhs are released from local sources and act at a distance on target cells that express the Hh receptor Patched. However, morphogen secretion and spreading are not passive processes because all Hhs are synthesized as dually (N- and C-terminal) lipidated proteins that firmly tether to the surface of producing cells. On the cell surface, Hhs associate with each other and with heparan sulfate (HS) proteoglycans. This raises the question of how Hh solubilization and spreading is achieved. We recently discovered that Sonic hedgehog (Shh) is solubilized by proteolytic processing (shedding) of lipidated peptide termini in vitro. Because unprocessed N termini block Patched receptor binding sites in the cluster, we further suggested that their proteolytic removal is required for simultaneous Shh activation. In this work we confirm inactivity of unprocessed protein clusters and demonstrate restored biological Shh function upon distortion or removal of N-terminal amino acids and peptides. We further show that N-terminal Shh processing targets and inactivates the HS binding Cardin-Weintraub (CW) motif, resulting in soluble Shh clusters with their HS binding capacities strongly reduced. This may explain the ability of Shh to diffuse through the HS-containing extracellular matrix, whereas other HS-binding proteins are quickly immobilized. Our in vitro findings are supported by the presence of CW-processed Shh in murine brain samples, providing the first in vivo evidence for Shh shedding and subsequent solubilization of N-terminaltruncated proteins.

The proteins of the Hedgehog (Hh)³ family are powerful

morphogens that control growth and patterning at various

developmental stages. In vertebrates, the function of Sonic

Hedgehog (Shh), one of the three members of the Hh protein family (Shh, Indian Hh, and Desert Hh), has been thoroughly

characterized (for review, see Ref. 1). Shh is essential for patterning of the ventral neural tube (2), for specifying vertebrate

digit identities (3, 4), and for the control of axon guidance in the

developing nervous system (5). Given these various functions, it

is not surprising that down-regulation of Hh signaling leads to

severe developmental abnormalities. In the adult, Hh pathway

activation is involved in maintaining the stem cell niche, includ-

ing the cancer stem cell niche (6), and Hh activity up-regulation

and subsequent release of the protein in multimeric form (18). The second lipid adduct that modifies Hh proteins is palmitic



contributes to the formation and progression of various cancers (6-8). Thus, tight control of Hh secretion and spreading is essential, and its molecular characterization required to better understand how Hh signals elicit dose-dependent responses in temporally and spatially specific manner. The Hh spreading mechanism is especially intriguing, because all Hh family members are released from producing cells despite being synthesized as dually lipid-modified, insoluble molecules (9). Both in vertebrates and in *Drosophila mela*nogaster, Hh synthesis starts with precursor proteins that undergo a series of post-translational modifications (10). After cleavage of an N-terminal signal peptide, Hh proteins undergo intein-related processing that involves internal cleavage between residues Gly-198 and Cys-199 (mouse Shh nomenclature) (11–14) and covalent attachment of a cholesteryl adduct to Gly-198 of the Shh signaling domain (11, 15–17). This mod-

^{*}This work was supported by German Research Council (DFG) Grant SFB 492-B15 and a Heinrich-Hertz fellowship (to K.G.) and DFG fellowship GRK1549/1 (to S. O., S. B., and U. P.).

This article contains supplemental Figs. 1–4.

¹ Both authors contributed equally to this work.

²To whom correspondence should be addressed. Fax: 49-251-8355596; E-mail: kgrobe@uni-muenster.de.

ification results in protein multimerization on the cell surface

³ The abbreviations used are: Hh, Hedgehog; Shh, Sonic Hedgehog; ShhNp, Shh N-terminal processed signaling domain; mShhNp, murine ShhNp; ADAM, a disintegrin and metalloprotease; Ptc, Patched; CW, Cardin-Weintraub; AP, alkaline phosphatase; M β CD, methyl- β -cyclodextrin; HS, heparan sulfate; HSPG, HS proteoglycan; sAP, secreted alkaline phosphatase.

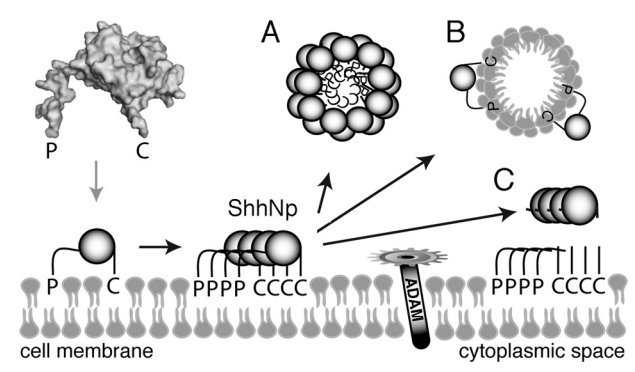


FIGURE 1. Proposed models for Hh release from producing cells. Human and mouse Shh signaling domains differ by only one amino acid, and their PDB structures are highly similar. This allowed us to combine murine Shh (PDB ID 1VHH, amino acids 39-195) and human Shh (PDB ID 3M1N, amino acids 25-190) to visualize both terminal, extended peptides (top left). Both terminal peptides are lipidated in vitro and in vivo, resulting in ShhNp tethering to cell membranes and morphogen multimerization via electrostatic protein-protein interactions. Classic models of Hh solubilization suggest detachment of lipidated morphogens from the membrane via micelle formation (A) or association of lipidated proteins with the phospholipid monolayer of lipoprotein particles (B). Alternatively, membrane-proximal cleavage of lipidated extended peptides by A disintegrin and metalloprotease (ADAM) sheddases results in the solubilization of truncated, biologically active ShhNp multimers in vitro (C). P, N-terminally linked palmitic acid; C, C-terminally linked cholesterol. Drawing not to scale.

acid, which attaches to the conserved N-terminal cysteine (Cys-25 in murine Shh) via the primary amine exposed after signal peptide cleavage (19). This unusual N-acylation is catalyzed by the product of the skinny hedgehog (Ski) gene (also designated sightless, central missing, raspberry, or Hh acyltransferase (20-23)). Although this hydrophobic modification would be expected to further decrease solubility (and thus morphogen diffusion), palmitoylation is absolutely required for Hh biological activity; unpalmitoylated multimeric proteins are $10-30 \times$ less active than N-palmitoylated wild-type forms (21, 24). The questions of how Hh lipidation and activity are linked and how dually lipid-modified Hhs are released from producing cells and spread through the extracellular compartment are currently under intense debate. So far, Hh release has been explained by lipid-dependent micelle formation, co-transport with lipoprotein particles, or ectodomain solubilization via proteolytic removal of both terminal, lipidated peptides (18, 25–27) (summarized in Fig. 1).

In the latter scenario, dually lipidated Shh multimers (from here on called ShhNp, standing for Shh N-terminal processed signaling domains) are released from transfected cells via ADAM (a disintegrin and metalloprotease)-mediated ectodomain shedding (18, 25). Shedding, however, does not only remove both lipidated peptide anchors but also activates ShhNp ectodomains in the process. Initially, on the cell surface, ShhNp N-terminal peptides interact with adjacent ShhNp zinc coordination sites in the cluster, thereby blocking Patched (Ptc) receptor binding to these sites (Fig. 2A) (18, 28-30). This renders the surface-tethered molecule inactive. By removing N-terminal acylated peptides, ADAMs expose Ptc binding zinc coordination sites and thereby couple ShhNp release with its biological activation. The established role of N-palmitoylation for the biological activity of secreted Hhs (21) is, therefore, indirect; N-acylation merely serves to anchor inhibitory N-terminal

peptides to the cell membrane as a prerequisite for their subsequent sheddase-mediated removal. Thus, any absence of N-palmitoylation (in the respective acyltransferase-deficient mutant or by site-directed mutagenesis of the acceptor cysteine residue into a serine (C25S mutagenesis in mouse ShhNp^{C25S})) restricts sheddase activity toward the C terminus and results in the release of inactive protein clusters with their zinc coordination sites (the Ptc binding sites) still blocked. The indirect role of N-acylation for ShhNp function is strongly supported by restored biological activity of otherwise inactive ShhNp^{C25S} upon N-terminal deletion mutagenesis (artificial truncation of the unpalmitoylated protein to mimic processing) (18). This suggests that N-palmitate does not directly contribute to receptor binding on receiving cells, at least in vitro.

In this work we further support these findings. First, we show that in addition to N-terminal deletion mutagenesis, insertional mutagenesis as well as forced proteolytic processing restore biological activities of otherwise inactive ShhNp^{C25S} (31). We also demonstrate that the N-terminal Cardin-Weintraub (CW) motif (32, 33) is processed during sheddase-mediated ShhNp release in vitro and in vivo. Because this motif contributes to ShhNp/HS interactions (30, 34, 35), CW-processing strongly reduces HS binding of truncated proteins. On the basis of these findings, we suggest that sheddase-mediated ShhNp release is coupled to functional morphogen activation and impaired HS binding of solubilized clusters, resulting in their facilitated diffusion into the HS-rich extracellular compartment.

MATERIALS AND METHODS

Mice-Endogenous murine (m)ShhNp was isolated from forebrains of 8-week-old C57/Bl6 mice (n = 6). Brains were separately homogenized in 20 mm Tris/HCl, pH 8.0, 137 mm NaCl, and 10% glycerol and subjected to ultracentrifugation. mShhNp in supernatants was then analyzed by heparin and heparan sulfate affinity chromatography (below) in three independent experiments. Additionally, all six cleared homogenates were concentrated via heparin-agarose pulldown or 5E1-immunoprecipitation (also described below). Precipitates were washed, and binding of Shh-specific antibodies 5E1 and α CW analyzed by immunoblotting. All experimental procedures were done in accordance with Society for Neuroscience and European Union guidelines.

Cloning and Expression of Recombinant Proteins-Shh constructs were generated from murine cDNA (NM 009170) using primers carrying the desired point mutations or deletions by PCR. PCR products (nucleotides 1-1314, corresponding to amino acids 1-438) were ligated into pDrive (Qiagen), sequenced, and subsequently released and religated into pcDNA3.1 (Invitrogen) for the expression of secreted, lipidated 19-kDa ShhNp in Bosc23 cells or HEK293 cells. PCR products (nucleotides 1-594, corresponding to amino acid 1-198 of murine Shh) were also cloned into pcDNA3.1 for expression of unlipidated 19-kDa ShhN in Bosc23 cells. Where indicated, a hemagglutinin (HA) tag was inserted between N-terminal amino acids Gly-32 and Lys-33 by site-directed mutagenesis (Stratagene), resulting in internally HA-tagged ShhNp. ShhNp^{C25S} (Cys-25 is required for N-terminal palmitoylation during release (18)) was generated by site-directed mutagenesis



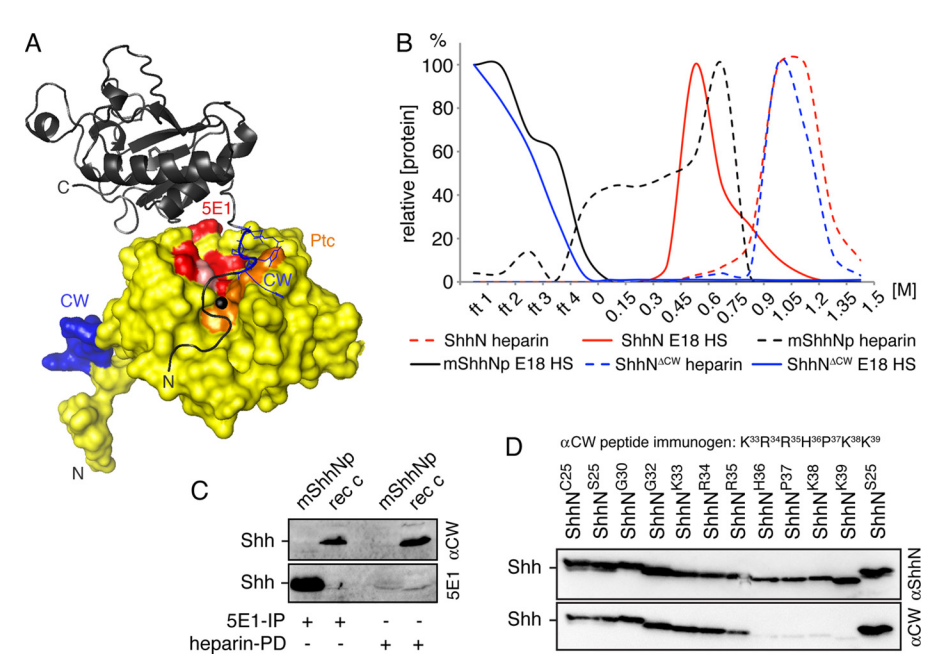


FIGURE 2. **Endogenous secreted mShNp is N-terminally processed.** *A*, Intermolecular interactions observed in the human ShhN crystal structure (PDB ID 3M1N) (18, 39). The N-terminal peptide of one molecule (black ribbon) overlaps 5E1 and Ptc binding sites of the adjacent molecule in the cluster (in yellow). 5E1 binding depends on Shh residues Thr-125, Asp-147, Arg-153, Ser-177, Ala-179, and His-180 (shown in red) (31). Ptc binding residues are shown in orange, and residue His-180 is bound by both 5E1 and Ptc, in pink. The α CW antibody-reactive CW peptide 35 RHPKK³⁹ is colored blue. Polyclonal α ShhN binds to multiple, undefined epitopes. *N*, N termini (C25). *C*, C terminus, *B*, ionic heparin- and E18-HS interactions of mouse brain-derived mShhNp and recombinant wild-type (ShhN) and CW-deficient ($ShhN^{\Delta CW}$) proteins are shown. For HS affinity chromatography, E18 embryonic HS was coupled to a FPLC column, proteins were applied, and bound proteins were eluted with a linear (0 – 1.5 m) NaCl gradient. All proteins bound to heparin; in contrast, only ShhN bound to HS. ShhN $^{\Delta CW}$ and mShhNp were both detected in the flow-through (ft), suggesting that the endogenous protein lacked functional HS binding CW residues. *C*, mShhNp and recombinant control proteins were concentrated by heparin-agarose pulldown in the presence of 0.5 m NaCl to suppress weak ionic interactions or 5E1 immunoprecipitation (IP). As shown in B, heparin bound the recombinant protein but not endogenous mShhNp, again indicating loss of basic amino acids. Consistent with this, immunoprecipitated mShhNp was 5E1-reactive but lacked α CW-antibody reactivity in all assays (n = 6). One representative experiment is shown. n = 6 proteins (N-terminal amino acids are indicated, n = 6 proteins were expressed and concentrated by heparin pulldown followed by immunoblotting. All truncated proteins were expressed at high levels, as indicated by polyclonal α ShNN reactivity. However, α CW-specific antibodies failed to

(Stratagene). N-terminally truncated forms and ShhNp 5xA or ShhNp $^{\Delta CW}$ (both lacking HS-binding Cardin-Weintraub function) were likewise generated by site-directed mutagenesis and sequenced. Primer sequences can be provided upon request. Constructs used in this study are presented in supplemental Fig. 1.

Cell Culture and Protein Analysis-Human Bosc23 or HEK293 cells were cultured in DMEM (PAA) with 10% fetal calf serum (FCS) and 100 μg/ml penicillin/streptomycin and were transfected using PolyFect (Qiagen). Cells were then kept for 36 h before the medium was harvested. In most assays, mutated or wild-type ShhNp were secreted into serum-containing or serum-free media without any additional treatment. Proteins secreted into serum-containing media were enriched by heparin-Sepharose (Sigma) pulldown overnight. Where indicated, methyl- β -cyclodextrin (Sigma) was used at 300 and 600 μ g/ml in serum-free DMEM. Proteins secreted into serum-free media were trichloroacetic acid (TCA)-precipitated. All proteins were analyzed by 15% SDS-PAGE followed by Western blotting using PVDF membranes. Immunodetection was conducted using polyclonal αShhN (goat IgG; R&D Systems), monoclonal 5E1 (DSHB, University of Iowa, USA)(36), or polyclonal α CWantibodies directed against the HS binding Cardin-Weintraub sequence (rabbit IgG, Cell Signaling) for primary protein detection. Visualization was performed after incubation with peroxidase-conjugated donkey- α -goat, α -mouse, or α -rabbit IgG (Dianova) followed by chemiluminescent detection (Pierce). For radiolabeling, 1 mCi of [9,19(n)-³H]palmitic acid was added to Shh-transfected HEK293 cells cultured in 35-mm dishes for 28 h under serum-free conditions before ShhNp release overnight. [³H]Palmitic acid-labeled cells as well as the harvested media were subjected to heparin-Sepharose pulldown to improve the signal to noise ratio. After SDS-PAGE, gels were immunoblotted, and the same blot was analyzed by autoradiography.

Chromatography—Proteins were purified by FPLC (Äkta Protein Purifier (GE Healthcare)) at 4 °C. Gel filtration analysis was performed using a Superdex200 10/300 GL column (GE Healthcare) equilibrated with PBS at 4 °C. Eluted fractions were TCA-precipitated, resolved by 15% SDS-PAGE, and immunoblotted. Signals were quantified using ImageJ. To determine HS binding of endogenous and recombinant forms of Shh, mouse brain lysates or supernatants of Shh-transfected Bosc23 cells were subjected to HS affinity chromatography (Äkta Protein Purifier). HS columns were generated as follows; embryonic day (E) 18 mouse embryos were digested overnight with 2 mg/ml Pronase in 320 mm NaCl, 100 mm sodium acetate, pH 5.5, at 40 °C, diluted 1:3 in water, and applied to 2.5 ml of DEAE Sephacel columns. glycosaminoglycan chains were applied to PD-10 (Sephadex G25) columns (GE Healthcare). Glycosami-

noglycans were lyophilized, again purified on DEAE as described above, applied to PD-10 columns, and again lyophilized. Via the peptides attached to the HS chains, samples were coupled to an NHS-activated Sepharose column according to the manufacturer's protocol (GE Healthcare). Proteins were applied to the column in the absence of salt, and bound material was eluted with a linear NaCl gradient from 0 to 1 M or 1.5 M in 0.1 M sodium acetate buffer, pH 6.0. Fractions were TCA-precipitated, resolved by 15% SDS-PAGE, and immunoblotted. The same E18 HS column was used for all experiments shown in this work.

Shh Reporter Assays—C3H10T1/2 cells (37) were grown in DMEM supplemented with 10% FCS and antibiotics. 24 h after seeding, Shh-conditioned media were mixed 1:1 with DMEM containing 10%FCS and antibiotics and applied to C3H10T1/2 cells in 15-mm plates. To some assays, 2.5 µg/ml 5E1 function blocking antibodies were added (36). Generally, because of variable expression levels, mutant and wild-type proteins required adjustment to comparable levels before induction of C3H10T1/2 differentiation. For adjustment, proteins were detected by immunoblotting, and detected bands were quantified by ImageJ. Cells were lysed 5-6 days after induction (20 mm Hepes, 150 mm NaCl, 0.5% Triton X-100, pH 7.4) and osteoblast-specific AP activity was measured at 405 nm after the addition of 120 mM p-nitrophenol phosphate (Sigma) in 0.1 M glycine buffer, pH 9.5. Assays were performed in triplicate.

Chondrocytes were isolated from the cranial third of 17-dayold chick embryo sterna by overnight digestion with collagenase and cultured in agarose suspension cultures under serumfree conditions. Cells were suspended in 0.5% low melting agarose in DMEM and allowed to sediment on the culture dishes that were precoated with 1% high melting agarose in water. Cells were grown at densities of 2 imes 10 6 cells/ml in DMEM mixed 1:1 with conditioned, serum-free medium from Shh-expressing cells. Media also contained 60 μ g/ml β -aminopropionitrile fumarate, 25 μg/ml sodium ascorbate, 1 mm cysteine, 1 mM pyruvate, 100 units/ml penicillin, and 100 μ g/ml streptomycin. After 14 days in culture, newly synthesized chondrocyte proteins were metabolically labeled with 1µCi/ml [14C]proline (250 Ci/mmol, PerkinElmer Life Sciences) for 24 h. Collagens were isolated after limited digestion with pepsin and were analyzed by SDS-PAGE followed by fluorography

5E1 Immunoprecipitation—10 μg of monoclonal 5E1 antibodies were coupled to 2.5 mg of Protein A-Sepharose beads (Sigma) per immunoprecipitation. 500 µl to 1 ml of lysate or medium were incubated overnight on a rotator and analyzed by SDS-PAGE and immunoblotting. For pulldown controls, 40 μ l of heparin-Sepharose beads were added to 500 μ l to 1 ml of Shh-containing media and incubated overnight on a rotator. Experiments were performed in triplicate.

Immunohistochemical Detection-sAP-ShhN and mutant forms generated by site-directed mutagenesis were cloned into gWIZ-SEAP (Gene Therapy Systems, San Diego, CA), expressed in Bosc23 cells, and secreted into the medium. Conditioned media were normalized for sAP activity and applied to 4% paraformaldehyde-fixed frozen embryonic day (E)12 mouse embryo sections overnight followed by 3 washes with PBS. sAP-

ShhN bound to HS was directly visualized by the addition of NBT-BCIP (Roche Applied Science). Control slides were heparinase I-III digested (IBEX, Montreal, Canada) (50 mm Hepes, 100 mm NaCl, 1 mm CaCl₂, 5 μg of BSA/ml, pH 7.0) at room temperature overnight to confirm Shh/HS specificity. sAP-ShhN was also incubated in the presence of 1 M NaCl to prove Shh/HS specificity.

Statistical Analysis—All statistical analysis was performed in Prism using Student's t test (two-tailed, unpaired, confidence interval 95%). All error estimates are S.D.

Molecular Modeling-The crystal structure of human Shh (PDB 3M1N)(39) was displayed employing the PyMOL Molecular Graphics System, Version 1.3, Schrödinger, LLC.

RESULTS

Isolation of N-terminal-truncated ShhNp from Mouse Brain— In our model of Shh release, sheddase-mediated processing of inhibitory N-terminal peptides is directly linked to biological activation of solubilized protein clusters. Unprocessed N-palmitoylated peptides (Fig. 2A, black ribbon) otherwise interact with zinc coordination sites of adjacent molecules in the cluster (yellow molecule, zinc is shown as a black sphere). Because Shh zinc coordination sites represent binding sites for the Shh receptor Ptc (colored in orange)(28,29), unprocessed N termini prevent receptor binding and thereby render the protein inactive. In this scenario, palmitate facilitates shedding via membrane-proximal positioning of N-terminal inhibitory peptides as a prerequisite for processing and also prevents solubilization of any incompletely activated (partially processed) morphogen clusters via their firm attachment to the cell membrane.

To confirm these in vitro derived data, we aimed to detect ShhNp processing in vivo. To this end, brain samples from 8-week-old C57/Bl6 mice were lysed in detergent-free buffer and centrifuged to deplete membrane-tethered murine (m) ShhNp. We then assessed binding of the soluble protein to physiologically relevant HS (Fig. 2B). To this end, HS derived from E18 C57/Bl6 mouse embryos was coupled to a HiTrap column, and protein binding was analyzed by FPLC affinity chromatography. The soluble fraction was also subjected to heparin affinity chromatography. Recombinant ShhN and mutant ShhN^{\(\Delta\)}CW lacking the HS binding CW motif served as positive and negative controls, respectively. Consistent with previous observations, control ShhN eluted from HS at 0.6 M NaCl and from heparin at 1 M NaCl (30). In contrast, brainderived 5E1-reactive mShhNp (40) did not bind to HS but eluted from heparin at 0 – 0.75 M NaCl. In this regard, endogenous mShhNp resembled ShhN $^{\Delta CW}$, which also binds heparin but not HS (30, 35). This suggested that endogenous, mouse brain-derived mShhNp lacks functional CW residues required for HS binding of the solubilized morphogen.

This finding prompted us to directly confirm loss of N-terminal CW residues during release. Murine brain samples were homogenized in detergent-free buffer and subjected to ultracentrifugation. Soluble mShhNp in supernatants was then incubated with agarose-linked heparin in the presence of 0.5 M NaCl to reduce unspecific interactions or immunoprecipitated using protein A-Sepharose-coupled 5E1 antibodies (supplemental Fig. 2A). Like Ptc,



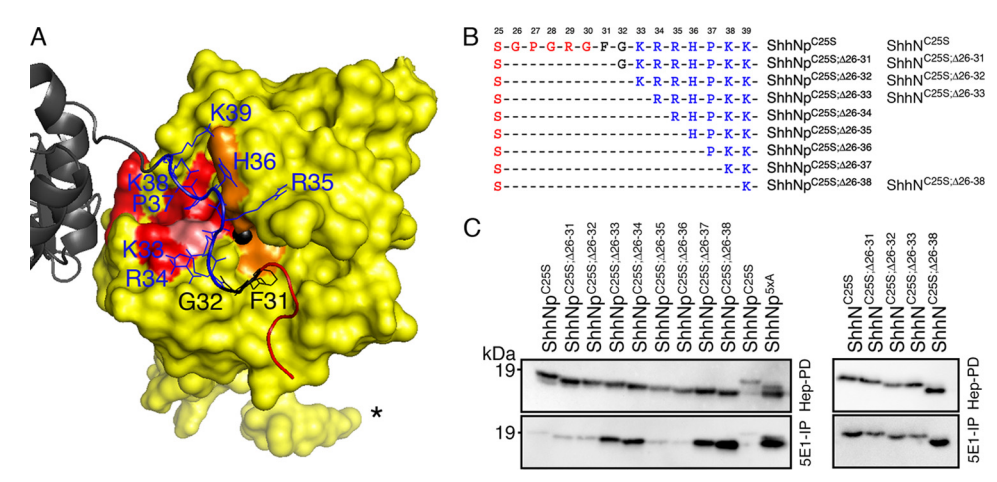


FIGURE 3. **ShhNp**^{C255} **N-terminal truncation restores 5E1 binding.** *A*, intermolecular interactions were observed in the human Shh crystal structure. The 5E1 binding site is shown in *red*, the Ptc binding site is in orange, and residue His-180 is bound by 5E1 and Ptc, in *pink*. N-terminal amino acids blocking these sites are labeled. *B*, all mutant proteins lack N-terminal Cys-25, preventing palmitoylation, and also variable numbers of N-terminal amino acids. *Red*, Ski/Hh acyltransferase recognition motif. *Blue*, CW-motif. *C*, ShhNp^{C255} and N-terminally truncated forms were expressed in Bosc23 cells, and soluble proteins were either 5E1-immunoprecipitated (*5E1-IP*) or concentrated by heparin-Sepharose pulldown. Proteins were immunoblotted and detected by α ShhN antibodies. Consistent with a previous report, 5E1 failed to immunoprecipitate ShhNp^{C255} (18). Consecutive N-terminal truncations, however, resulted in restored 5E1 binding, especially of ShhNp^{C255}, A26-37</sup>, ShhNp^{C255}, A26-38, and ShhNp^{C255}, A26-39. Proteolytically processed ShhNp^{SxA} served as a positive control (30). *Right*, corresponding monomeric proteins (ShhN) were N-terminally truncated and analyzed as described above (*B*, *right*). Comparable 5E1 binding of truncated and untruncated monomers confirms Shh clustering as a prerequisite for protein inactivation in *trans*.

monoclonal 5E1 binds the Shh zinc coordination site (Fig. 2A, 5E1 epitope is in *red*), residue histidine 180 being bound by both the receptor and the antibody (Fig. 2A, pink) (31). 5E1 binding thus competes with Ptc binding (thereby inhibiting Shh signaling) (36), and ShhNp binding of the antibody and the receptor is blocked by unprocessed N-terminal peptides (18). As a conseguence, 5E1 binds N-terminally truncated ShhNp but not the unprocessed precursor. For subsequent Shh detection, we employed SDS-PAGE and PVDF immunoblotting using αCW antibodies raised against the N-terminal peptide immunogen ³³KRRHPKK³⁹ (the CW motif). The same blot was then stripped and incubated with 5E1 antibodies. Both antibody specificities were confirmed using recombinant Shh controls (supplemental Fig. 2, B and C). Consistent with impaired HS binding shown in Fig. 2B, 5E1-reactive endogenous proteins were clearly detected in the immunoprecipitated material but not after heparin pulldown (Fig. 2C). Notably, 5E1-immunoreactive mShhNp on the same (stripped) blot lacked α CW-antibody reactivity, in contrast to recombinant control proteins. Thus, results shown in Fig. 2, B and C, suggest N-terminal processing of solubilized mShhNp in vivo.

As an approximation for the N-terminal mShhNp processing site, we next determined minimum requirements for α CW antibody binding. To this end, we employed artificially truncated forms of recombinant ShhN that lacked variable numbers of N-terminal amino acids and determined that amino acids 35 RHPKK 39 were required and sufficient for α CW antibody binding to soluble proteins (Fig. 2*D*, residues are colored *blue* in *A*, and supplemental Fig. 2*C*). The observed lack of mShhNp α CW antibody reactivity thus suggests processing of endogenous proteins at arginine 35 or downstream residues.

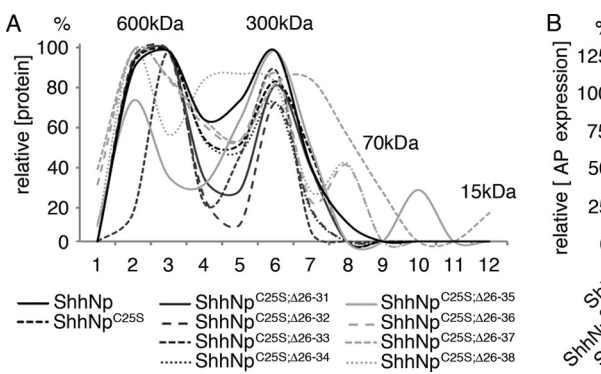
Notably, proteolytic CW processing is consistent with two published findings. 1) Site-directed exchange of all five basic CW residues for alanines (ShhNp^{5xA}) increases morphogen processing (30), indicating cleavage susceptibility of this site in the absence of bound HS. 2) Automated Edman degradation of

Escherichia coli-expressed Shh revealed two potential CW cleavage sites, CGPGRGFG $\underline{K}^{33} \downarrow \underline{RRHPKK}LTPLAY...$ (CW residues are underlined, \downarrow denotes the processing site) and CGPGRGFG $\underline{KRRHPK}^{38} \downarrow \underline{KLTPLAY...}$ (25). Importantly, N-terminal CW residues are conserved in all vertebrate Hh family members, raising the possibility that this site represents a general sheddase target site. Unfortunately, multiple attempts to N-terminally sequence soluble proteins from *in vivo* sources or transfected cells *in vitro* failed because of insufficient Shh recovery after purification (data not shown).

N-terminal ShhNp^{C25S} Truncation Restores 5E1 Binding— Therefore, we established alternative strategies to identify N-terminal ShhNp processing sites in vitro. One strategy involved recombinant expression of unpalmitoylated (and thus, N-terminally unprocessed) ShhNp^{C25S} in addition to engineered variants that lacked variable numbers of N-terminal amino acids (Fig. 3, A and B). The underlying idea was that expression of 5' truncated cDNA lacking codons for Shh amino acids 26-38 would mimic N-terminal processing and thus restore 5E1 binding of otherwise unreactive ShhNp^{C25S}. To this end, secreted proteins were either 5E1-immunoprecipitated or pulled down using heparin-Sepharose beads that bind all forms (30). We indeed detected strong heparin binding of all proteins (Fig. 3C, top blot, left) but found that ShhNp^{C25S}, ShhNp^{C25S;Δ26-35}, and ShhNp^{C25S;Δ26-36} were not 5E1-immunoprecipitated (Fig. 3C, bottom blot, left). In contrast, 5E1-binding of ShhNp $^{C25S;\Delta26-37}$, ShhNp^{C25S;Δ26-38}, ShhNp^{C25S;Δ26-34}, and ShhNp^{C25S;Δ26-34} was fully restored, as it was comparable to ShhNp^{5xA} serving as a positive control (30). Further analysis confirmed blocked 5E1 binding in trans because 5E1-binding of monomeric ShhN^{C25S} and truncated monomers ShhN^{C25S;\Delta26-31}, ShhN^{C25S;\Delta26-32}, ShhN^{C25S;\Delta26-33}, and ShhN^{C25S;\Delta26-38} was comparable (Fig. 3*C*, *right*).

N-terminal $ShhNp^{C2SS}$ Truncation Restores Ptc Binding— Thus, to rule out false positive results due to the possible release of monomeric truncated $ShhNp^{C2SS}$ variants, we confirmed





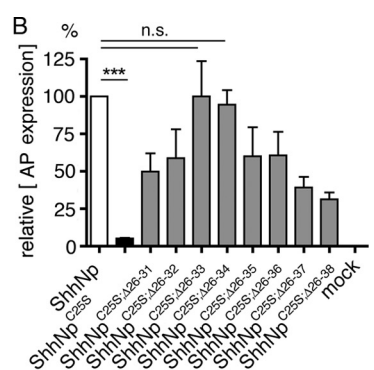


FIGURE 4. Restored biological activity of N-terminally truncated, palmitoylation-deficient ShhNp^{C25S} variants. All mutant proteins lacked N-terminal C25, preventing palmitoylation, in addition to consecutive N-terminal peptides (Fig. 3B). Comparable amounts of mutated proteins were employed in all the following assays, as determined by immunoblotting. A, comparable 600- and 100 –300-kDa multimerization was detected by gel filtration of ShhNp^{C255} and compound mutant proteins (ShhNp^{C255; Δ 26-31} to ShhNp^{C255; Δ 26-38}). Elution profiles are expressed relative to the highest protein level in a given run, which was set to 100%. B, C3H10T1/2 osteoblast precursor cells were incubated with single and compound mutant proteins, and the relative amount of Shh-induced AP production was determined as a biological readout. Medium obtained from mock-transfected Bosc23 cells and ShhNp^{C255}-conditioned medium were used as negative controls, and ShhNp conditioned medium was used as a positive control (set to 100%, other values were expressed relative to ShhNp activity). In this assay, ShNNp^{C255},(226-33) and ShNnp^{C255},(226-34) showed activities comparable with that of the wild type (103 \pm 20% and 99.5 \pm 11% relative to the wild-type control, p=0.9 and 0.94, n=6). All truncated ShNnp^{C255} double mutants showed significantly increased biological activities if compared with non-truncated ShNnp^{C255} (p<0.05) in all forms). *** denote significant ShNnp activity if compared with ShNnp^{C255} (p<0.01). n.s., not significant (p>0.05).

their unimpaired multimerization by gel filtration (Fig. 4A). Unimpaired multimerization of all forms allowed us to subsequently conduct biological tests as a readout for their Ptc binding capacities. To this end, we took advantage of Shh-dependent C3H10T1/2 osteoblast precursor cell differentiation as a sensitive bioassay (37). As shown in Fig. 4B, wild-type control ShhNp strongly induced C3H10T1/2 differentiation into alkaline phosphatase (AP)-producing osteoblasts. In contrast, negative control media obtained from mock-transfected Bosc23 cells as well as full-length ShhNp^{C25S} were inactive as expected. In agreement with restored 5E1 binding shown before, we observed variable C3H10T1/2 differentiation induced by truncated ShhNp $^{\text{C25S}}$ variants; here, ShhNp $^{\text{C25S};\Delta26-33}$ and ShhNp^{C25S;\Delta 26-34} showed strongest relative activities (control ShhNp activity was set to 100%, Fig. 4B). ShhNp $^{\text{C25S};\Delta26-34}$ also induced Gli1-dependent firefly luciferase expression in Light-2 cells (41) and led to Shh-dependent differentiation of primary chondrocytes (38) (supplemental Fig. 3). However, we noticed that induced C3H10T1/2 and Light-2 activities varied considerably, possibly due to the presence of serum factors or unspecific effects of N-terminal serine 25 replacing the palmitate acceptor cysteine. Yet, variable but restored biological activities observed in all three assays indicate preferred processing at, or close to, CW residues Arg-34/35 during ShhNp release in vitro.

Forced N-terminal Processing also Restores ShhNp^{C25S} Bioactivity—A more robust test for processing-dependent Shh biofunction involved incubation of transfected HEK293 cells with 300 and 600 μ g/ml methyl- β -cyclodextrin (M β CD), a cyclic oligosaccharide that depletes cholesterol from living cells. Under serum-free conditions, M β CD strongly increases ShhNp release (25) in agreement with M β CD acting as a sheddase stimulator. Fig. 5A shows N-terminally processed ShhNp (double asterisks) generated from the cell-tethered precursor protein (single asterisk) (42–47). MβCD-induced shedding targeted CW residue Arg-35 or downstream residues, as indicated by reduced α CW-antibody reactivity of the bottom (processed) band (same stripped blot, double asterisks denote the processed form). This observation confirms ShhNp release via MβCD- activated sheddases, because any possible direct extraction of molecules via their cholesteryl moiety should have left their molecular weight and α CW antibody reactivity unchanged.

MβCD treatment of ShhNp^{C25S}-transfected HEK293 cells also resulted in increased morphogen solubilization (via stimulated processing of membrane-linked C termini) as expected. Notably, this treatment also resulted in N-terminal protein processing (Fig. 5A, double asterisks), in contrast to normal culture conditions that always produced soluble intact ShhNp^{C25S} (Fig. 5A, left). Based on our model of coupled N-terminal processing and activation (Figs. 3C and 4B), we expected increased bioactivity of M β CD-released ShhNp^{C25S} over the unprocessed form (18, 21, 24, 27, 48-50). As shown in Fig. 5B, released ShhNp^{C25S} in the presence of 300 μ g/ml M β CD indeed stimulated C3H10T1/2 cells (1.1 \pm 0.2 arbitrary units (ShhNp^{C25S}) *versus* 1.34 ± 0.06 arbitrary units (ShhNp), p = 0.1919, relative activity ratio 1.3:1, n = 4). In contrast, ShhNp^{C25S} expressed under normal conditions (in the presence of FCS, no M β CD) failed to significantly differentiate C3H10T1/2 cells (0.32 ± 0.001 arbitrary units versus 0.97 ± 0.018 arbitrary units obtained for ShhNp, $p \le 0.0001$, n = 4 (Fig. 5*B*)). Correction for the mock value (0.24 arbitrary units) resulted in an ShhNp/ ShhNp^{C25S} activity ratio of 10:1. 1.55 \pm 0.23 arbitrary units were obtained after incubation with 600 μ g/ml M β CD (ShhNp^{C25S}) compared with 2.1 ± 0.14 arbitrary units for the wild type, p = 0.062, n = 4 (ShhNp/ShhNp^{C25S} activity ratio, 1.44:1). Control MβCD treatment of mock-transfected HEK293 cells did not induce C3H10T1/2 differentiation. We draw two conclusions from this experiment. First, restored ShhNp^{C25S} bioactivity demonstrates that N-palmitate is not directly required for ShhNp signaling on receiving cells, consistent with previous in vitro findings (Fig. 4B). Second, restored bioactivity of N-processed ShhNp^{C25S} is consistent with restored 5E1 binding and signaling pathway activation shown in Figs. 3C and 4B and supplemental Fig. 3, confirming coupled ShhNp N-terminal truncation and functional activation.

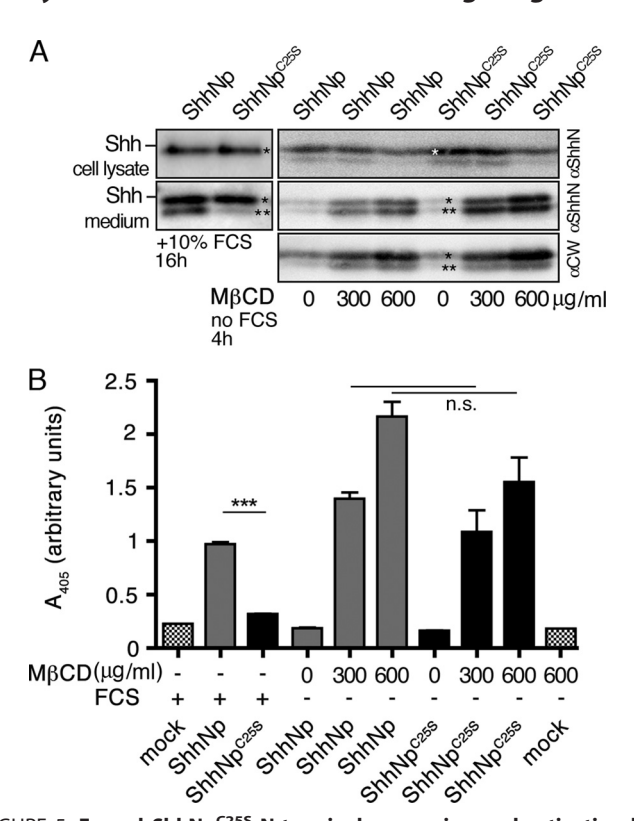


FIGURE 5. Forced ShhNp^{C25S} N-terminal processing and activation by MBCD. A, 40 h after HEK293 cells were transfected with full-length Shh cDNA or cDNA encoding for the palmitoylation-deficient protein, cells were washed, and serum-free DMEM with or without 300 and 600 $\mu \mathrm{g/ml}$ M β CD was added. After 4 h, the medium was harvested, and subjected to centrifugation and TCA precipitation followed by SDS-PAGE and Western blot analysis using α ShhN and α CW antibodies. Cellular protein expression levels (cell lysates) are shown on top. Right, M β CD treatment resulted in forced shedding and increased release of N-terminally truncated ShhNp and ShhNp^{C25S} into supernatants. Reduced α CW reactivity of processed proteins indicates cleavage at or in close vicinity to CW residue Arg-35 (bottom blot). Results from the same (*stripped*) blot are shown. *Left*, control expression of N-terminally truncated ShhNp (*double asterisks*) and unprocessed ShhN^{C255} (*asterisk*) in the presence of 10% FCS and without M β CD are shown. B, C3H10T1/2 osteoblast precursor cells were incubated with aliquots of the same ShhNp and ShhNp^{C255}-conditioned media analyzed above, and relative amounts of Shhinduced AP-activity were determined. Medium from mock-transfected HEK293 cells was used as a control. *** denote significance between biological activities of ShhNp and unprocessed ShhNp C255 expressed without M β CD (p < 0.01). In contrast, the observed difference between M β CD-released ShhNp and ShhNp^{C25S} was insignificant (n.s., p > 0.05).

Insertional Mutagenesis also Restores ShhNp^{C25S} Bioactivity— Additional support for regulatory roles of N-terminal peptides was obtained by insertional mutagenesis. HA-tagged proteins (N-terminal peptide sequence (C/S)GPGRGFGYPYDVPDY-AKRRHPKK³⁹ (underlined letters represent the tag, supplemental Fig. 1)) were expressed, and the soluble proteins were tested for their biological activities (18). As a control, media from untransfected Bosc23 cells failed to induce C3H10T1/2 differentiation (mock), and ShhNp C25S activity was $\sim 30 \times$ reduced if compared with untagged wild-type proteins (2.8 \pm 0.11 arbitrary units (ShhNp) versus 0.18 \pm 0.016 (ShhNp^{C25S}), p = 0.0001, n = 4) (Fig. 6A). These findings confirm our previous results (Fig. 5B) and those of others (19, 51). In contrast, we noticed that biological activities of HA-tagged ShhNp^{C25S} were only ~2× reduced if compared with HA-tagged wild-type proteins under the same experimental conditions (1.62 \pm 0.05 arbitrary units (ShhNp_{HA}) versus 0.85 ± 0.03 (HA-tagged

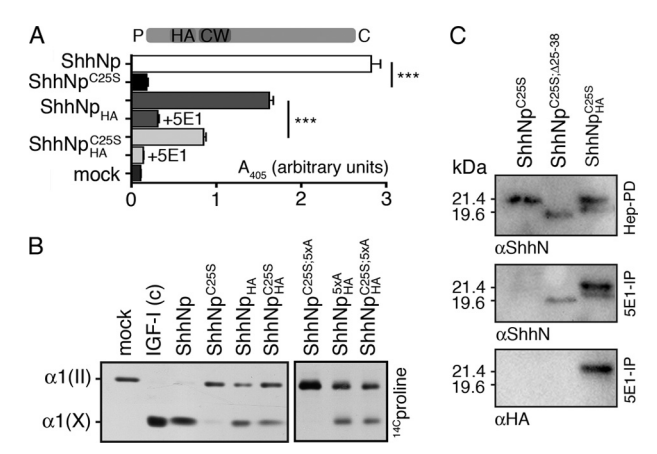


FIGURE 6. ShhNp^{C25S} insertional mutagenesis restores 5E1 binding and biological activity. A, C3H10T1/2 osteoblast precursor cells were incubated with comparable amounts of untagged and HA-tagged (top, P indicates palmitate, C indicates cholesterol) wild-type and unpalmitoylated ShhNp^{C25S} produced in DMEM+10% FCS. The relative amounts of Shh-induced AP activity were determined as a readout for C3H10T1/2 differentiation and hence for biological activity of the proteins. Medium obtained from mock-transfected Bosc23 cells served as a negative control. For ShhNp and ShhNp^{C25S}, differences in biological activity were always significant (ShhNp^{C25S}, 0.18 ± 0.017 arbitrary units, versus ShhNp, 2.815 \pm 0.11 arbitrary units, p < 0.0001, n = 4; ShhNp/ShhNp $^{\text{C25S}}$ activity ratio, \sim 30 \times). The relative activity of HA-tagged ShhNp cases, however, was greatly increased if compared with HA-tagged ShhNp (HA-tagged ShhNp cases) \pm 0.03 arbitrary units, versus HA-tagged ShhNp, 1.62 \pm 0.05 arbitrary units, p = 0.0086, n = 4; ShhNp/ShhNp^{C25S} activity ratio; \sim 2 \times). *** denote significance (p < 0.01). B, serum-free conditioned media were added to primary chick chondrocytes (38). Differentiation of these cells was monitored by [14 Ć]proline incorporation into collagen II ($\alpha 1(II)$) and collagen X ($\alpha 1(X)$) after 14 days in culture, as analyzed by 14 C autoradiography. Chondrocyte hypertrophy (as indicated by α 1(X) production) was induced by HA-tagged ShhNp^{C255} in the presence or absence of the CW motif (ShhNp^{5xA}) but not by untagged ShhNp^{C255}. Insulin-like growth factor I (*IGF-I*) and ShhNp served as positive controls, and the media of mock-transfected Bosc23 cells served as the negative control. C, secreted proteins were 5E1-immunoprecipitated or concentrated by heparin-Sepharose pulldown and immunoblotted. ShhNp^{C255} was 5E1-unreactive (negative control), and truncated ShhNp^{C255}; \(\text{\text{\text{2}}} \) was 5E1-reactive (positive control as shown in Fig. 3C)). Fulllength HA-ShhNp^{C255} was 5E1-immunoprecipitated, indicating that the HA tag disturbed the location of inhibitory peptides in the cluster.

ShhNp^{C25S}), p = 0.0001, n = 4). Co-incubation with Shh-neutralizing 5E1 antibodies resulted in strong inhibition of both observed activities, demonstrating specificity of the assay. We confirmed this result by Hh-dependent chondrocyte differentiation under serum-free conditions (38). In this bioassay, primary chick chondrocytes were incubated with ShhNp-conditioned media, and collagen X production was used as a readout for Hh-induced hypertrophic differentiation (Fig. 6B). Insulinlike growth factor I (IGF-I), ShhNp, and ShhNp_{HA} served as positive controls. In contrast, untagged ShhNp^{C25S} and ShhNp $^{ ext{C25S;5xA}}$ (lacking N-palmitoylation in addition to a functional CW motif) were always inactive, serving as negative controls. Notably, HA-tagged ShhNp^{C25S} induced prehypertrophic chondrocyte differentiation into collagen X-producing hypertrophic chondrocytes, and HA-tagged ShhNp^{C25S;5xA} was also active. These observations confirm Shh activity regulation by N-terminal peptides and that N-palmitate is not directly required for Shh biofunction on receiving cells. We hypothesized that the inserted nine-amino acid HA-tag disturbed peptide/protein contacts, resulting in facilitated Ptc binding of unprocessed clusters. To confirm this possibility, heparin-Sepharose pulldown and 5E1 immunoprecipitation of ShhNp^{C25S} and HA-tagged ShhNp^{C25S} were conducted as described above

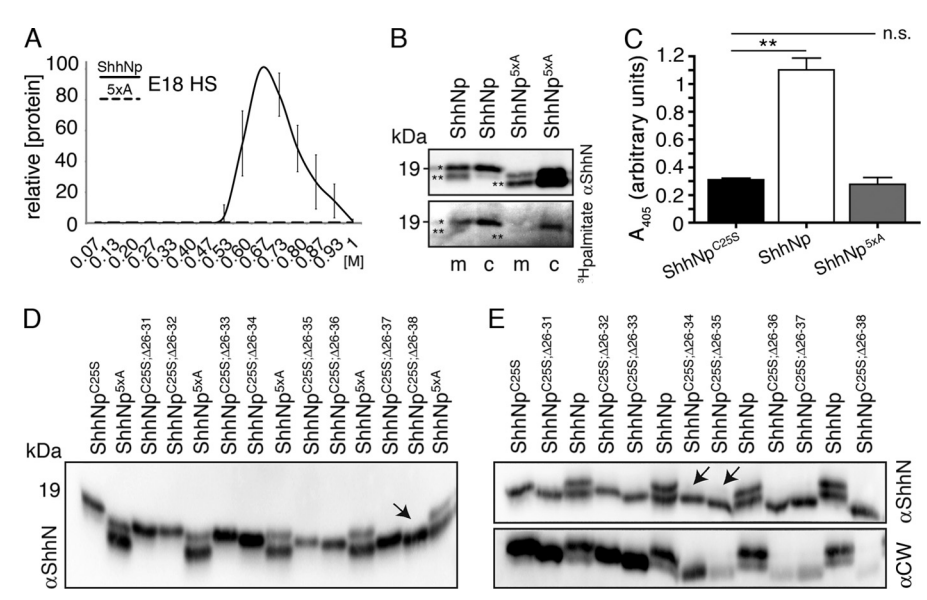


FIGURE 7. **CW mutagenesis abolishes HS-binding and increases ShhNp processing.** A, deletion of all five basic CW residues fully abolishes ShhNp 5xA binding to E18 embryo-derived HS. Averaged elution profiles of three independent ShhNp and ShhNp 5xA analyses on the same HS-coupled affinity column are shown. Error estimates are S.D. B, an immunoblot (top) and autoradiograph (bottom) of [9,10(n)- 3 H]palmitic acid-labeled, full-length ShhNp and ShhNp 5xA in cell lysates (c) and media (m) are shown. Full-length 19-kDa ShhNp (asterisk) was detected in lysates and media by Western blotting and ³H autoradiography. Unprocessed, radiolabeled ShhNp^{5xA} was also detected in the cell lysate. In contrast, truncated soluble ShhNp and ShhNp^{5xA} (double asterisks) derived from the labeled cell-bound forms lacked [³H]palmitic acid, indicating N-terminal processing. Note that relative processing of ShhNp^{5xA} was increased if compared with the wild-type protein. The presence of unprocessed soluble ShhNp in media is due to extensive cell death caused by serum-free culture conditions required for labeling. C, C3H10T1/2 osteoblast precursor cell differentiation is significantly induced by processed ShNp but not by unprocessed ShNpC²⁵⁵ (1.1 \pm 0.08 arbitrary units versus 0.3 \pm 0.01 arbitrary units, n = 6, p = 0.0023). In this assay, ShNpS^{5xA} was inactive despite its N-terminal processing (0.27 \pm 0.05 arbitrary units, p = 0.57 compared with ShNpC²⁵⁵). ** denote significance; n.s., not significant (p > 0.05). D, size comparison of processed ShNNpS^{5xA} with ShNpC²⁵⁵ and N-terminally truncated proteins is shown. Comparable size of ShNpC²⁵⁵, $\Delta 26^{-38}$ demonstrates cleavage or close to position 37 (arrow). E, shown is analysis of ShNPC²⁵⁵, $\Delta 26^{-38}$ demonstrates cleavage or close to position 37 (arrow). E, shown is analysis of ShNPC²⁵⁵, $\Delta 26^{-38}$ demonstrates cleavage of $\Delta 26^{-38}$ demonstrates cleavage or $\Delta 26^{-38}$ demonstrates cleavage of $\Delta 26^{-38}$ demonstrates cleavage or $\Delta 26^{-38}$ demonstrates $\Delta 2$ ShhNp, as described in D. In contrast to ShhNp sxA, ShhNp is cleaved at or in proximity to position 34/35 (arrows), as confirmed by reduced α CW antibody reactivity of processed proteins.

(Fig. 3C), and PVDF-blotted proteins were analyzed by α ShhN and α HA-directed antibodies. ShhNp^{C25S; Δ 26-38} served as a positive (5E1 binding) control (Fig. 3C). As shown in Fig. 6C, top, HA-tagged and untagged ShhNp^{C25S} bound to heparin. Protein A-coupled 5E1, however, immunoprecipitated only HA-tagged ShhNp^{C25S} but not the untagged form. Based on these findings, we conclude that insertional mutagenesis rescues $ShhNp^{C25S}$ biofunction by rearranging inhibitory peptides away from the Ptc binding zinc coordination site.

Site-directed CW Mutagenesis Facilitates N-terminal ShhNp Processing—Next, we investigated the possibility that ShhNp activation in vitro depends on proteolytic processing of specific, "permissive" N-terminal target sites. Based on the observed loss of α CW antibody reactivity during processing, the HS binding CW motif may represent one such target. To test this idea, we compared ShhNp and ShhNp5xA processing and release, the latter construct lacking all five basic CW residues. This abolished ShhNp^{5xA} binding to HiTrap column-coupled E18 embryo-derived HS, as assessed by FPLC (Fig. 7A) (30, 33). We next aimed to directly confirm ShhNp depalmitoylation during processing and release. To this end, ShhNp- and ShhNp^{5xA}transfected HEK293 cells were grown in the presence of [9,10(n)-3H]palmitic acid for specific N-terminal radiolabeling. Soluble and cell-bound proteins were harvested and PVDF-immunoblotted; the same blot was then subjected to autoradiography to detect C25-linked [3H]palmitic acid. As shown in Fig. 7B, cell-tethered 19-kDa proteins (top bands, single asterisk) were labeled and largely unprocessed, consistent with their [³H]palmitic acid signals. These bands represented the dually

lipidated morphogens. In contrast, increased electrophoretic mobility ShhNp^{5xA} protein signals lacked [³H]palmitic acid (Fig. 7B, bottom, double asterisks), thus representing the N-terminally processed proteins (Fig. 3C). Notably, in this assay ShhNp processing was strongly reduced if compared with ShhNp^{5xA}. Because CW residues associate with cell-surface HS before release (52), this observation suggests that HS binding may (down)regulate sheddase-mediated processing and release, possibly via blockade of susceptible CW residues.

Interestingly, we observed that processed ShhNp^{5xA} was inactive in C3H10T1/2 cells (Fig. 7C, 0.27 ± 0.05 arbitrary units, p = 0.57 compared with ShhNp^{C25S}, 0.3 ± 0.01 arbitrary units, n = 5). In contrast, ShhNp was always active (1.1 \pm 0.08 arbitrary units, p = 0.0023 if compared with ShhNp^{C25S}, n = 5). As a possible explanation, we hypothesized that ShhNp^{5xA} could have been processed at a "non-permissive" site different from the wild-type site (Fig. 4B). We employed two alternative strategies to test this idea. First, molecular weight analysis of unprocessed versus processed ShhNp^{5xA} using Bio1D software revealed an ~1400-Da size shift corresponding to N-terminal residues ²⁵CGPGRGFGKRRHP³⁷ (1405 Da). This suggested peptide cleavage between Pro-37 and Lys-38. Second, we immunoblotted N-truncated ShhNp C25S mutants (Fig. 3, B and C) together with ShhNp 5xA . As shown in Fig. 7D, the processed ShhNp^{5xA} protein (bottom band) corresponded in size with ShhNp^{C25S;\D26-38} (arrow), confirming the processing site. Lys-38 processing is consistent with robust 5E1 reactivity of the protein (Fig. 3C) but low bioactivity of corresponding ShhNp^{C25S}-truncated mutants in C3H10T1/2 cells (Figs. 4B



and 7*C*). In contrast, Arg-34/35 processing was linked to ShhNp release (Fig. 7*E*, top blot), consistent with impaired α CW binding of processed proteins (Fig. 7*E*, bottom blot), strong 5E1 binding of corresponding ShhNp^{C25S; Δ 26-34} (Fig. 3*C*), and restored ShhNp^{C25S; Δ 26-34} and ShhNp^{C25S; Δ 26-35} biological activities in C3H10T1/2 cells (Fig. 4*B*). Based on these findings and those of others (25), we suggest cleavage of CW residues Arg-34/35 as a requirement for ShhNp solubilization and activation.

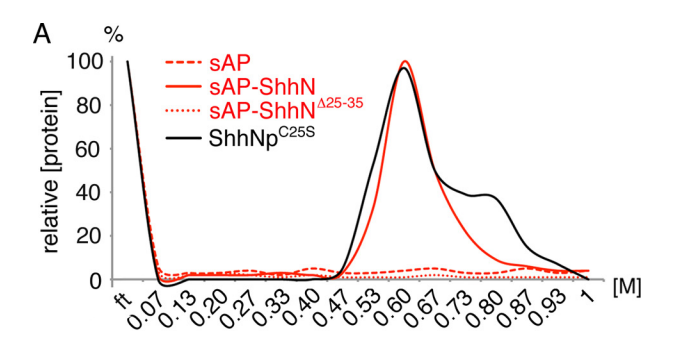
HS Binding of CW-processed Shh Is Reduced—Because HS/Shh interactions are CW-dependent, as shown in this work and elsewhere (30, 33, 35), and because HSPGs are critically involved in Shh biology (53–58), we aimed to confirm that CW processing at or beyond residue 35 reduces protein binding to HS (Fig. 2B). This would provide an explanation for the ability of solubilized ShhNp to travel a long distance in the HS-containing extracellular compartment (56, 59–62), effectively escaping HS-mediated protein immobilization and internalization.

To test this possibility, we first compared binding of processed and unprocessed proteins to FPLC column-coupled E18-derived HS (Fig. 2B) (30). We first compared ionic interactions of ShhNp^{C25S} (the N-terminally unprocessed multimer) with the unprocessed, alkaline phosphatase (sAP)-tagged monomeric protein (sAP-ShhN). Both proteins eluted at 0.6 M NaCl, demonstrating comparable HS binding of monomeric and multimeric unprocessed proteins (Fig. 8A). Control sAP did not bind HS, demonstrating specificity of the assay. Next, comparable AP-activities of sAP, sAP-ShhN, and CW-truncated sAP-ShhN $^{\Delta25-35}$ were applied to the same E18 HS-column, and sAP activities in the flow-through were monitored to confirm saturation of HS binding sites. Here, in notable contrast to strong sAP-ShhN binding to HS (30), sAP-ShhN $^{\Delta25-35}$ did not bind to E18 HS. This confirmed CW-dependent Shh/HS binding in vitro and that CW truncation impairs Shh association with physiologically relevant forms of HS, such as embryonic HS.

An embryonic tissue known to be patterned by Shh is the developing neural tube. To directly test this tissue, E12 embryo sections were incubated with equal amounts of the same sAP, sAP-ShhN, and sAP-ShhN $^{\Delta25-35}$ proteins used above. As a readout for Shh binding to tissue HS, sAP activity was detected colorimetrically (Fig. 8B) (34). sAP-ShhN yielded a strong signal, and negative controls sAP and sAP-ShhNp^{5xA}, HS digestion with heparinase I-III before sAP-ShhN incubation, or sAP-ShhN incubation in the presence of 1 M NaCl demonstrated CW-dependent, specific HS binding of the protein. As expected, sAP-ShhN $^{\Delta25-35}$ failed to bind HS on tissue sections. Based on this and previous results, we conclude that HS/ShhN interactions depend on the CW motif (30, 34, 35) and that CW processing during release reduces HS binding of solubilized proteins. Conversion of HS-associated cell surface clusters into soluble unreactive forms may thus underlie unimpaired extracellular ShhNp diffusion.

DISCUSSION

How morphogen gradients arise has attracted much controversy. So far, micelle formation and lipoprotein-mediated



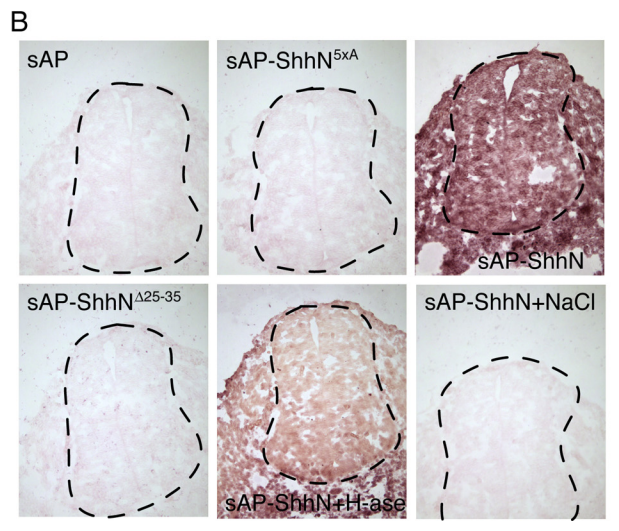


FIGURE 8. **CW-truncated ShhN does not bind to HS.** A, ionic E18-HS interactions of mono- and multimeric proteins are shown. HS binding of unprocessed multimeric ShhNp^{C255} was comparable with that of alkaline phosphatase (sAP)-tagged sAP-ShhN, the latter representing the directly secreted, unlipidated monomer. Equal amounts of sAP control protein and CW-truncated sAP-ShhN $^{\Delta 26-35}$, as determined by comparable AP-activity in both samples, were applied to the same E18-HS column, and sAP activities in the flowthrough (ft) confirmed saturation of Shh binding sites on the column. In contrast to sAP-ShhN, no sAP and sAP-ShhN $^{\Delta 25-35}$ elution could be observed, demonstrating strongly impaired HS binding of the N-terminally truncated protein. B, sAP-ShhN ligand binding to horizontal embryonic neural tube (dashed line) sections is shown. Paraformaldehyde-fixed E12 mouse embryos were sectioned and treated with equal amounts of sAP and sAP-ShhN 5xA control proteins, sAP-ShhN $^{\Delta 25-35}$, wild-type sAP-ShhN, and sAP-ShhN in the presence of 1 M NaCl or heparinase (H-ase) I-III to remove cell surface HS. Bound sAP-ShhN was detected by its sAP activity upon incubation with NBT-BCIP. In contrast, the truncated CW mutant did not bind to HS.

transport, morphogen transport by transcytosis (the sequential endocytosis and exocytosis of bound ligands (63)), and transport via "bucket brigade" (receptor-bound morphogen on one cell moves by being handed over to receptors on adjacent cells (64)) have been suggested. One major argument against extracellular Hh morphogen diffusion, which would represent another possible mechanism, was its apparent incompatibility with dual ShhNp lipidation and hydrophobicity. However, as confirmed in this work, ShhNp shedding represents a mechanism to overcome this problem. Another major argument against morphogen diffusion was that cell surface receptors or non-receptors, such as HSPGs, would strongly impair extracellular movement of "sticky" molecules. Indeed, extracellular glypicans represent a major group of Hh-binding HSPGs that modulate morphogen activity, mobility, and stability (53, 57, 58, 65-67). Here, negatively charged HS chains represent the main direct interactors between HSPGs and highly conserved



CW motifs present in all Hhs (30, 33, 35). The resulting Hh/HS interactions are essential for Hh multimerization on producing cells (52); however, similar interactions in the HSPG-rich extracellular matrix would be expected to prevent long-range diffusion of soluble proteins (64, 68).

In this work we suggest that CW processing during release resolves this problem via conversion of HS binding surface proteins into unreactive soluble clusters. This mechanism would allow for unimpaired HSPG/ShhNp interactions on the cell surface, yet facilitate protein diffusion upon removal of essential CW amino acids. Therefore, we postulate that cell-surface shedding serves three functions in Hh biology; it is required for the solubilization of cell surface-linked morphogen clusters, their biological activation during release, and their associated reduction of HS binding. We are aware of the possibility that N-terminal peptides may get cleaved at different CW amino acids during release, possibly resulting in variable HS binding of alternatively truncated soluble proteins. In addition to variable HS binding, N-terminal Shh processing at different sites may also predetermine biological responses of receiving cells (Fig. 4 and supplemental Fig. 3) at the molecular level. This is indicated by alternative transcriptional activities of responding C3H10T1/2 cells after stimulation with differently truncated ShhNp, as shown in supplemental Fig. 4. Thus, alternative N-terminal processing may represent a new regulator for the various biological responses that Shh can elicit. Interestingly, and consistent with this idea, N-terminal proteolysis also specifically regulates biological activities of secreted Wnt morphogens. Wnt family members are essential for embryogenesis, pathogenesis, and regeneration, and like Hhs, palmitoylated Wnt proteins initially locate to the cell surface and require solubilization to reach their targets. In this process, Wnts can undergo proteolysis-induced processing of eight N-terminal amino acids, resulting in Wnt oxidation oligomerization and functional inactivation (69). Therefore, Wnts and Shh represent two examples for the emerging theme of functional morphogen control by proteolytic removal of regulatory N-terminal peptides.

In contrast to proteolysis-induced Wnt inactivation, however, removal of ShhNp N termini activates the oligomerized protein (40). This is supported by restored ShhNp^{C25S} biofunction and 5E1 binding after deletion mutagenesis, as shown in this work. Furthermore, enhanced N-terminal processing in the presence of M β CD is associated with increased electrophoretic mobility, associated loss of α CW-reactivity, and biological activation of truncated ShhNp and ShhNp^{C25S}. Notably, these observations may be reflected by recently demonstrated bioactivity of HEK293-expressed, 5E1-immunoprecipitated lower molecular weight ShhNp, and the lack of such an activity in the remaining higher molecular weight protein (Fig. 6 in Ref. 70). Because we and others showed that higher molecular weight ShhNp is palmitoylated, in contrast to increased electrophoretic mobility ShhNp (the bottom band), which is not (Fig. 7B) (70), we conclude that N-acylation, although essential for ShhNp biological activity per se, is not directly involved in ShhNp signaling on receiving cells. This confutes the third argument against sheddase-dependent morphogen diffusion; that is, the assumed direct role of N-palmitate for Hh bioactivity.

Instead, we suggest that N-palmitate ensures quantitative N-terminal ShhNp processing as a prerequisite for complete activation of all solubilized molecules, as incompletely processed clusters will remain tethered to the cell surface. As a consequence, protein concentrations at any position in the responsive field correlate with their biological activities (their Ptc binding capacities). In contrast, in the absence of quantitative N-terminal processing, biological activities of solubilized clusters would vary, depending on the relative number of processed N-terminal peptides. As a result, protein concentrations at any position in the field would not reliably correlate with Shh signaling activities. This in turn would affect morphogen-dependent tissue patterning in unpredictable ways. In the most extreme case, e.g. in acyltransferase-deficient mutants, processing would be restricted to C-terminal peptides in the cluster, resulting in the solubilization of inactive proteins and complete decoupling of protein/activity gradients. This essential "cleavage/activation control" function may explain the unusual attachment of palmitate via an amide bond to the α -amino group of all Hhs, whereas palmitate in most other proteins is thioester (S)-linked (71). S-Linked palmitate, however, is susceptible to enzymatic deacylation by palmitoyl-protein thioesterases, which would result in a situation comparable with that in acyltransferase-deficient mutants. In contrast, amide-linked palmitate is resistant to thioesterase activity and thus restricts possible modes of Hh release to shedding, ensuring the release of fully activated proteins. As discussed above, N-palmitoylation may simultaneously ensure quantitative CW processing and inactivation required for unimpaired ShhNp diffusion through the matrix. Endogenous expression of 5E1-reactive but αCW antibody and HS-unreactive mShhNp in the in vivo mouse brain strongly supports this idea.

Acknowledgments—We acknowledge analysis of Light2 cells by Susanne Höing (Max-Planck Institute for Molecular Biomedicine, Münster, Germany). The 5E1 antibody developed by T. M. Jessell was obtained from the Developmental Studies Hybridoma Bank maintained by the University of Iowa, Iowa City, Iowa. The excellent technical and organizational assistance of Sabine Kupich is gratefully acknowledged.

REFERENCES

- 1. McMahon, A. P., Ingham, P. W., and Tabin, C. J. (2003) Developmental roles and clinical significance of hedgehog signaling. Curr. Top. Dev. Biol. **53,** 1–114
- 2. Briscoe, J., Chen, Y., Jessell, T. M., and Struhl, G. (2001) A hedgehoginsensitive form of patched provides evidence for direct long-range morphogen activity of sonic hedgehog in the neural tube. Mol. Cell 7, 1279 - 1291
- 3. Ahn, S., and Joyner, A. L. (2004) Dynamic changes in the response of cells to positive hedgehog signaling during mouse limb patterning. Cell 118,
- 4. Harfe, B. D., Scherz, P. J., Nissim, S., Tian, H., McMahon, A. P., and Tabin, C. J. (2004) Evidence for an expansion-based temporal Shh gradient in specifying vertebrate digit identities. Cell 118, 517–528
- 5. Charron, F., Stein, E., Jeong, J., McMahon, A. P., and Tessier-Lavigne, M. (2003) The morphogen sonic hedgehog is an axonal chemoattractant that collaborates with netrin-1 in midline axon guidance. Cell 113, 11-23



- Zhao, C., Chen, A., Jamieson, C. H., Fereshteh, M., Abrahamsson, A., Blum, J., Kwon, H. Y., Kim, J., Chute, J. P., Rizzieri, D., Munchhof, M., VanArsdale, T., Beachy, P. A., and Reya, T. (2009) Hedgehog signalling is essential for maintenance of cancer stem cells in myeloid leukaemia. *Nature* 458, 776–779
- Theunissen, J. W., and de Sauvage, F. J. (2009) Paracrine Hedgehog signaling in cancer. Cancer Res. 69, 6007–6010
- Yauch, R. L., Gould, S. E., Scales, S. J., Tang, T., Tian, H., Ahn, C. P., Marshall, D., Fu, L., Januario, T., Kallop, D., Nannini-Pepe, M., Kotkow, K., Marsters, J. C., Rubin, L. L., and de Sauvage, F. J. (2008) A paracrine requirement for hedgehog signalling in cancer. *Nature* 455, 406 – 410
- Peters, C., Wolf, A., Wagner, M., Kuhlmann, J., and Waldmann, H. (2004)
 The cholesterol membrane anchor of the Hedgehog protein confers stable membrane association to lipid-modified proteins. *Proc. Natl. Acad. Sci. U.S.A.* 101, 8531–8536
- Mann, R. K., and Beachy, P. A. (2004) Novel lipid modifications of secreted protein signals. *Annu. Rev. Biochem.* 73, 891–923
- Liu, X. Q. (2000) Protein-splicing intein. Genetic mobility, origin, and evolution. Annu. Rev. Genet. 34, 61–76
- Lee, J. J., Ekker, S. C., von Kessler, D. P., Porter, J. A., Sun, B. I., and Beachy,
 P. A. (1994) Autoproteolysis in hedgehog protein biogenesis. *Science* 266, 1528–1537
- 13. Tabata, T., and Kornberg, T. B. (1994) Hedgehog is a signaling protein with a key role in patterning *Drosophila* imaginal discs. *Cell* **76**, 89–102
- Bumcrot, D. A., Takada, R., and McMahon, A. P. (1995) Proteolytic processing yields two secreted forms of sonic hedgehog. *Mol. Cell. Biol.* 15, 2294–2303
- Porter, J. A., Young, K. E., and Beachy, P. A. (1996) Cholesterol modification of hedgehog signaling proteins in animal development. *Science* 274, 255–259
- Porter, J. A., Ekker, S. C., Park, W. J., von Kessler, D. P., Young, K. E., Chen, C. H., Ma, Y., Woods, A. S., Cotter, R. J., Koonin, E. V., and Beachy, P. A. (1996) Hedgehog patterning activity. Role of a lipophilic modification mediated by the carboxyl-terminal autoprocessing domain. *Cell* 86, 21–34
- Martí, E., Bumcrot, D. A., Takada, R., and McMahon, A. P. (1995) Requirement of 19K form of Sonic hedgehog for induction of distinct ventral cell types in CNS explants. *Nature* 375, 322–325
- Ohlig, S., Farshi, P., Pickhinke, U., van den Boom, J., Höing, S., Jakuschev, S., Hoffmann, D., Dreier, R., Schöler, H. R., Dierker, T., Bordych, C., and Grobe, K. (2011) Sonic hedgehog shedding results in functional activation of the solubilized protein. *Dev. Cell* 20, 764–774
- Pepinsky, R. B., Zeng, C., Wen, D., Rayhorn, P., Baker, D. P., Williams, K. P., Bixler, S. A., Ambrose, C. M., Garber, E. A., Miatkowski, K., Taylor, F. R., Wang, E. A., and Galdes, A. (1998) Identification of a palmitic acid-modified form of human Sonic hedgehog. *J. Biol. Chem.* 273, 14037–14045
- Amanai, K., and Jiang, J. (2001) Distinct roles of Central missing and Dispatched in sending the Hedgehog signal. *Development* 128, 5119 –5127
- Chamoun, Z., Mann, R. K., Nellen, D., von Kessler, D. P., Bellotto, M., Beachy, P. A., and Basler, K. (2001) Skinny hedgehog, an acyltransferase required for palmitoylation and activity of the hedgehog signal. *Science* 293, 2080–2084
- Lee, J. D., and Treisman, J. E. (2001) Sightless has homology to transmembrane acyltransferases and is required to generate active Hedgehog protein. Curr. Biol. 11, 1147–1152
- Micchelli, C. A., The, I., Selva, E., Mogila, V., and Perrimon, N. (2002) Rasp, a putative transmembrane acyltransferase, is required for Hedgehog signaling. *Development* 129, 843–851
- Lee, J. D., Kraus, P., Gaiano, N., Nery, S., Kohtz, J., Fishell, G., Loomis, C. A., and Treisman, J. E. (2001) An acylatable residue of Hedgehog is differentially required in *Drosophila* and mouse limb development. *Dev. Biol.* 233, 122–136
- Dierker, T., Dreier, R., Petersen, A., Bordych, C., and Grobe, K. (2009) Heparan sulfate-modulated, metalloprotease-mediated sonic hedgehog release from producing cells. *J. Biol. Chem.* 284, 8013–8022
- Panáková, D., Sprong, H., Marois, E., Thiele, C., and Eaton, S. (2005) Lipoprotein particles are required for Hedgehog and Wingless signalling. Nature 435, 58–65

- Zeng, X., Goetz, J. A., Suber, L. M., Scott, W. J., Jr., Schreiner, C. M., and Robbins, D. J. (2001) A freely diffusible form of Sonic hedgehog mediates long-range signalling. *Nature* 411, 716–720
- Bishop, B., Aricescu, A. R., Harlos, K., O'Callaghan, C. A., Jones, E. Y., and Siebold, C. (2009) Structural insights into hedgehog ligand sequestration by the human hedgehog-interacting protein HHIP. *Nat. Struct. Mol. Biol.* 16, 698 –703
- Bosanac, I., Maun, H. R., Scales, S. J., Wen, X., Lingel, A., Bazan, J. F., de Sauvage, F. J., Hymowitz, S. G., and Lazarus, R. A. (2009) The structure of SHH in complex with HHIP reveals a recognition role for the Shh pseudo active site in signaling. *Nat. Struct. Mol. Biol.* 16, 691–697
- Farshi, P., Ohlig, S., Pickhinke, U., Höing, S., Jochmann, K., Lawrence, R., Dreier, R., Dierker, T., and Grobe, K. (2011) Dual roles of the Cardin-Weintraub motif in multimeric Sonic hedgehog. *J. Biol. Chem.* 286, 23608–23619
- 31. Maun, H. R., Wen, X., Lingel, A., de Sauvage, F. J., Lazarus, R. A., Scales, S. J., and Hymowitz, S. G. (2010) Hedgehog pathway antagonist 5E1 binds hedgehog at the pseudo-active site. *J. Biol. Chem.* **285**, 26570–26580
- 32. Cardin, A. D., and Weintraub, H. J. (1989) Molecular modeling of proteinglycosaminoglycan interactions. *Arteriosclerosis.* **9,** 21–32
- Rubin, J. B., Choi, Y., and Segal, R. A. (2002) Cerebellar proteoglycans regulate sonic hedgehog responses during development. *Development* 129, 2223–2232
- Chan, J. A., Balasubramanian, S., Witt, R. M., Nazemi, K. J., Choi, Y., Pazyra-Murphy, M. F., Walsh, C. O., Thompson, M., and Segal, R. A. (2009) Proteoglycan interactions with Sonic Hedgehog specify mitogenic responses. *Nat. Neurosci.* 12, 409 – 417
- Chang, S. C., Mulloy, B., Magee, A. I., and Couchman, J. R. (2011) Two distinct sites in sonic Hedgehog combine for heparan sulfate interactions and cell signaling functions. *J. Biol. Chem.* 286, 44391–44402
- Ericson, J., Morton, S., Kawakami, A., Roelink, H., and Jessell, T. M. (1996)
 Two critical periods of Sonic Hedgehog signaling required for the specification of motor neuron identity. *Cell* 87, 661–673
- Nakamura, T., Aikawa, T., Iwamoto-Enomoto, M., Iwamoto, M., Higuchi, Y., Pacifici, M., Kinto, N., Yamaguchi, A., Noji, S., Kurisu, K., and Matsuya, T. (1997) Induction of osteogenic differentiation by hedgehog proteins. *Biochem. Biophys. Res. Commun.* 237, 465–469
- Dreier, R., Günther, B. K., Mainz, T., Nemere, I., and Bruckner, P. (2008)
 Terminal differentiation of chick embryo chondrocytes requires shedding
 of a cell surface protein that binds 1,25-dihydroxyvitamin D3. *J. Biol. Chem.* 283, 1104–1112
- Pepinsky, R. B., Rayhorn, P., Day, E. S., Dergay, A., Williams, K. P., Galdes, A., Taylor, F. R., Boriack-Sjodin, P. A., and Garber, E. A. (2000) Mapping sonic hedgehog-receptor interactions by steric interference. *J. Biol. Chem.* 275, 10995–11001
- Dierker, T., Dreier, R., Migone, M., Hamer, S., and Grobe, K. (2009) Heparan sulfate and transglutaminase activity are required for the formation of covalently cross-linked hedgehog oligomers. *J. Biol. Chem.* 284, 32562–32571
- Taipale, J., Chen, J. K., Cooper, M. K., Wang, B., Mann, R. K., Milenkovic, L., Scott, M. P., and Beachy, P. A. (2000) Effects of oncogenic mutations in Smoothened and Patched can be reversed by cyclopamine. *Nature* 406, 1005–1009
- 42. Tellier, E., Canault, M., Rebsomen, L., Bonardo, B., Juhan-Vague, I., Nalbone, G., and Peiretti, F. (2006) The shedding activity of ADAM17 is sequestered in lipid rafts. *Exp. Cell Res.* **312**, 3969–3980
- Kojro, E., Gimpl, G., Lammich, S., Marz, W., and Fahrenholz, F. (2001) Low cholesterol stimulates the nonamyloidogenic pathway by its effect on the α-secretase ADAM 10. Proc. Natl. Acad. Sci. U.S.A. 98, 5815–5820
- von Tresckow, B., Kallen, K. J., von Strandmann, E. P., Borchmann, P., Lange, H., Engert, A., and Hansen, H. P. (2004) Depletion of cellular cholesterol and lipid rafts increases shedding of CD30. *J. Immunol.* 172, 4324–4331
- Walev, I., Tappe, D., Gulbins, E., and Bhakdi, S. (2000) Streptolysin Opermeabilized granulocytes shed L-selectin concomitantly with ceramide generation via neutral sphingomyelinase. *J. Leukoc. Biol.* 68, 865–872
- 46. Zimina, E. P., Bruckner-Tuderman, L., and Franzke, C. W. (2005) Shedding of collagen XVII ectodomain depends on plasma membrane mi-



- croenvironment. J. Biol. Chem. 280, 34019-34024
- 47. Matthews, V., Schuster, B., Schütze, S., Bussmeyer, I., Ludwig, A., Hundhausen, C., Sadowski, T., Saftig, P., Hartmann, D., Kallen, K. J., and Rose-John, S. (2003) Cellular cholesterol depletion triggers shedding of the human interleukin-6 receptor by ADAM10 and ADAM17 (TACE). J. Biol. Chem. 278, 38829 - 38839
- 48. Chen, M. H., Li, Y. J., Kawakami, T., Xu, S. M., and Chuang, P. T. (2004) Palmitoylation is required for the production of a soluble multimeric Hedgehog protein complex and long-range signaling in vertebrates. Genes Dev. 18, 641-659
- 49. Dawber, R. J., Hebbes, S., Herpers, B., Docquier, F., and van den Heuvel, M. (2005) Differential range and activity of various forms of the Hedgehog protein. BMC Dev. Biol. 5, 21
- 50. Kohtz, J. D., Lee, H. Y., Gaiano, N., Segal, J., Ng, E., Larson, T., Baker, D. P., Garber, E. A., Williams, K. P., and Fishell, G. (2001) N-terminal fattyacylation of sonic hedgehog enhances the induction of rodent ventral forebrain neurons. Development 128, 2351-2363
- 51. Buglino, J. A., and Resh, M. D. (2008) Hhat is a palmitoylacyltransferase with specificity for N-palmitoylation of Sonic Hedgehog. J. Biol. Chem. **283,** 22076 – 22088
- 52. Vyas, N., Goswami, D., Manonmani, A., Sharma, P., Ranganath, H. A., VijayRaghavan, K., Shashidhara, L. S., Sowdhamini, R., and Mayor, S. (2008) Nanoscale organization of hedgehog is essential for long-range signaling. Cell 133, 1214-1227
- 53. Bornemann, D. J., Duncan, J. E., Staatz, W., Selleck, S., and Warrior, R. (2004) Abrogation of heparan sulfate synthesis in *Drosophila* disrupts the Wingless, Hedgehog. and Decapentaplegic signaling pathways. Development 131, 1927-1938
- 54. Gallet, A., Staccini-Lavenant, L., and Thérond, P. P. (2008) Cellular trafficking of the glypican Dally-like is required for full-strength Hedgehog signaling and wingless transcytosis. Dev Cell 14, 712-725
- 55. Takei, Y., Ozawa, Y., Sato, M., Watanabe, A., and Tabata, T. (2004) Three Drosophila EXT genes shape morphogen gradients through synthesis of heparan sulfate proteoglycans. Development ${\bf 131,73}-82$
- 56. Gritli-Linde, A., Lewis, P., McMahon, A. P., and Linde, A. (2001) The whereabouts of a morphogen. Direct evidence for short- and graded longrange activity of hedgehog signaling peptides. Dev. Biol. 236, 364-386
- 57. Bellaiche, Y., The, I., and Perrimon, N. (1998) Tout-velu is a Drosophila homologue of the putative tumour suppressor EXT-1 and is needed for Hh diffusion. Nature 394, 85-88
- 58. The, I., Bellaiche, Y., and Perrimon, N. (1999) Hedgehog movement is regulated through tout velu-dependent synthesis of a heparan sulfate pro-

- teoglycan. Mol. Cell 4, 633-639
- Gallet, A., Ruel, L., Staccini-Lavenant, L., and Thérond, P. P. (2006) Cholesterol modification is necessary for controlled planar long-range activity of Hedgehog in Drosophila epithelia. Development 133, 407-418
- 60. Ayers, K. L., Gallet, A., Staccini-Lavenant, L., and Thérond, P. P. (2010) The long-range activity of Hedgehog is regulated in the apical extracellular space by the glypican Dally and the hydrolase Notum. Dev. Cell 18, 605 - 620
- 61. Caspary, T., García-García, M. J., Huangfu, D., Eggenschwiler, J. T., Wyler, M. R., Rakeman, A. S., Alcorn, H. L., and Anderson, K. V. (2002) Mouse Dispatched homolog1 is required for long-range, but not juxtacrine, Hh signaling. Curr. Biol. 12, 1628-1632
- 62. Lewis, P. M., Dunn, M. P., McMahon, J. A., Logan, M., Martin, J. F., St-Jacques, B., and McMahon, A. P. (2001) Cholesterol modification of sonic hedgehog is required for long-range signaling activity and effective modulation of signaling by Ptc1. Cell 105, 599-612
- 63. Entchev, E. V., Schwabedissen, A., and González-Gaitán, M. (2000) Gradient formation of the TGF- β homolog Dpp. Cell 103, 981–991
- 64. Kerszberg, M., and Wolpert, L. (1998) Mechanisms for positional signalling by morphogen transport. A theoretical study. J Theor. Biol. 191, 103 - 114
- 65. Han, C., Belenkaya, T. Y., Khodoun, M., Tauchi, M., and Lin, X. (2004) Distinct and collaborative roles of Drosophila EXT family proteins in morphogen signalling and gradient formation. Development 131, 1563-1575
- 66. Han, C., Belenkaya, T. Y., Wang, B., and Lin, X. (2004) Drosophila glypicans control the cell-to-cell movement of Hedgehog by a dynamin-independent process. Development 131, 601-611
- 67. Koziel, L., Kunath, M., Kelly, O. G., and Vortkamp, A. (2004) Ext1-dependent heparan sulfate regulates the range of Ihh signaling during endochondral ossification. Dev. Cell 6, 801-813
- Lander, A. D., Nie, Q., and Wan, F. Y. (2002) Do morphogen gradients arise by diffusion? Dev. Cell 2, 785-796
- 69. Zhang, X., Abreu, J. G., Yokota, C., MacDonald, B. T., Singh, S., Coburn, K. L., Cheong, S. M., Zhang, M. M., Ye, Q. Z., Hang, H. C., Steen, H., and He, X. (2012) Tiki1 is required for head formation via Wnt cleavageoxidation and inactivation. Cell 149, 1565-1577
- 70. Creanga, A., Glenn, T. D., Mann, R. K., Saunders, A. M., Talbot, W. S., and Beachy, P. A. (2012) Scube/You activity mediates release of dually lipidmodified Hedgehog signal in soluble form. Genes Dev. 26, 1312-1325
- 71. Resh, M. D. (2006) Trafficking and signaling by fatty-acylated and prenylated proteins. Nat. Chem. Biol. 2, 584-590

